Microscopic Mechanisms of Electric-Field-Induced Alignment of Block Copolymer Microdomains

A. Böker,[1] H. Elbs,[1] H. Hänsel,[1] A. Knoll,[1] S. Ludwigs,[1] H. Zettl,[1] V. Urban,[2] V. Abetz,[3] A. H. E. Müller,[3] and G. Krausch[1,*]

[1]*Lehrstuhl für Physikalische Chemie II, Bayreuther Zentrum für Kolloide und Grenzflächen, Universität Bayreuth, D-95440 Bayreuth, Germany*

[2]*European Synchrotron Radiation Facility (ESRF), F-38043 Grenoble, France*

[3]*Lehrstuhl für Makromolekulare Chemie II, Bayreuther Zentrum für Kolloide und Grenzflächen, Universität Bayreuth, D-95440 Bayreuth, Germany*

(Received 28 May 2002; published 4 September 2002)

We investigate the microscopic mechanisms responsible for microdomain alignment in block copolymer solutions exposed to an electric field. Using time-resolved synchrotron small-angle x-ray scattering, we reveal two distinct processes, i.e., grain boundary migration and rotation of entire grains, as the two dominant microscopic mechanisms. The former dominates in weakly segregating systems, while the latter is predominant in strongly segregated systems. The kinetics of the processes are followed as a function of polymer concentration and temperature and are correlated to the solution viscosity.

DOI: 10.1103/PhysRevLett.89.135502 PACS numbers: 61.10.–i

The spontaneous formation of nanostructured materials via molecular self-assembly has gained increasing interest throughout the past decade, driven both by its inherent beauty and by a wealth of potential technological applications. Incompatible block copolymers are a prominent example for this class of materials as they form a large variety of well ordered microdomain structures of molecular dimensions [1,2]. However, the self-assembly process typically leads to an isotropic multidomain structure of only short range order. The use of external fields has proven helpful to overcome this drawback and create macroscopically large monodomains. Most prominently, mechanical fields have been used to macroscopically orient block copolymers in melt [3–5] and solution [6,7].

Only recently, the potential of external electric fields has been exploited for microdomain alignment in block copolymer melt thin films [8]. Both lamellar and cylindrical microdomain structures were oriented macroscopically by virtue of a dc electric field [8–11]. Experiments in the melt, however, are limited by the high viscosities typical for high molecular weight copolymers or copolymers of more complex architectures. These limitations can be circumvented by using concentrated block copolymer solutions in nonselective solvents [12,13]. The key to an understanding of the reorientation behavior of block copolymer microdomains in solution is the knowledge of the underlying microscopic mechanisms contributing to the rearrangement of domains. In contrast to the case of shear alignment of block copolymers, which has been studied by a variety of different experimental techniques such as *in situ* birefringence [4], *in situ* small-angle neutron scattering [14], and *ex situ* small-angle x-ray scattering (SAXS) [15–17], only little is known about the relevant microscopic processes playing a role during block copolymer alignment in the presence of an electric field.

In the present Letter, we report on real-time SAXS experiments on concentrated block copolymer solutions aiming to study the kinetics of microdomain orientation in the presence of an electric field and thus to elucidate the underlying microscopic processes. Synchrotron-SAXS combines the advantages of the above-mentioned *in situ* techniques (high time resolution of 0.1 sec) with detailed information on the microscopic state of order, typical for a high quality scattering experiment. We identify two distinct microscopic mechanisms, each of which dominates the reorientation process in a certain regime of polymer concentration and temperature.

A polystyrene-*block*-polyisoprene (SI) diblock copolymer of nearly symmetric composition was synthesized by sequential living anionic polymerization. The polymer consists of 52 wt.% polystyrene (PS) and 48 wt.% polyisoprene (PI) with a total number-average molecular weight $M_n = 80\,000$ g/mol and a polydispersity $M_w/M_n = 1.02$. The polymer was dissolved in toluene with concentrations ranging from 30 to 80 wt.%. The alignment experiments were performed in a home-built capacitor with gold electrodes (electrode distance: 2 mm) at temperatures between 25 and 80 °C. A dc voltage of 2 kV was applied across the electrodes, resulting in a homogeneous electric field pointing perpendicular to the direction of the x-ray beam [see Fig. 1(a)]. No leakage currents were detected. Synchrotron-SAXS measurements were performed at the ID2A beam line at the European Synchrotron Radiation Facility (ESRF, Grenoble, France). The diameter of the x-ray beam was 200 μm. The photon energy was set to 12.5 keV. SAXS patterns were recorded with a two-dimensional camera located at a distance of 10 m from the sample within an

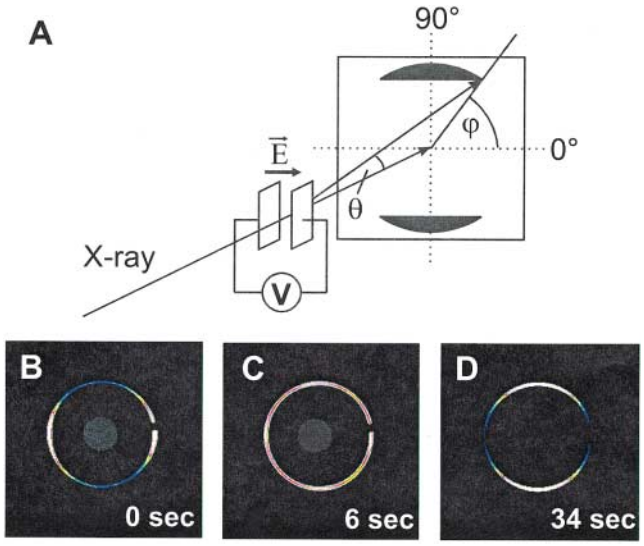

FIG. 1 (color). (A) Experimental setup for *in situ* SAXS. (B)–(D) Two-dimensional SAXS pattern of a 35 wt. % solution of a SI diblock copolymer in toluene taken at 25 °C prior to (B) and after application of an electric field ($E = 1$ kV/mm) (C),(D). The color scale in C is exaggerated for clarity [see Fig. 2(a)].

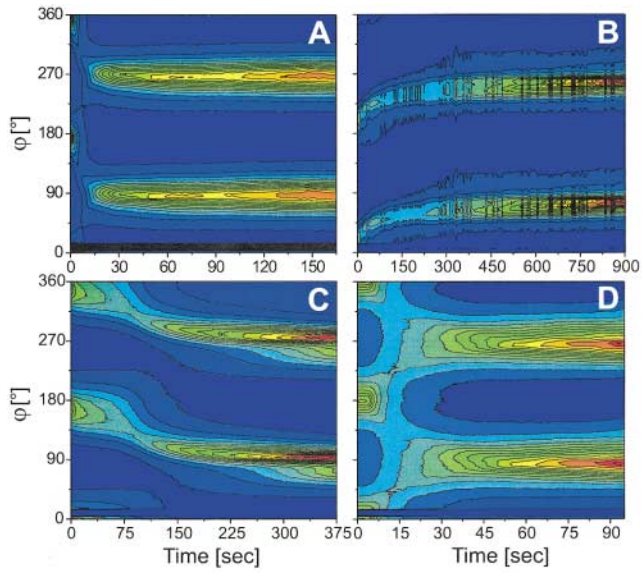

FIG. 2 (color). Time development of the scattering intensity as a function of the azimuthal angle φ in the presence of an electric field of strength $E = 1$ kV/mm for different polymer concentrations and temperatures. (A) $w_{pol} = 35$ wt. %, $T = 25$ °C; (B) $w_{pol} = 50$ wt. %, $T = 25$ °C; (C) $w_{pol} = 47.5$ wt. %, $T = 27$ °C; (D) $w_{pol} = 47.5$ wt. %, $T = 80$ °C.

evacuated flight tube. The detector can monitor up to 125 frames (1024 × 1024 pixels) at a rate of 10 frames per second.

In a first set of experiments (not shown here), we investigated the ordering behavior of the block copolymer solutions in the absence of an electric field. At room temperature, we found an order-disorder transition (ODT) at about $w_{pol, ODT} = 34.5$ wt. %, above which a well-defined lamellar microdomain structure is developed. A characteristic lamellar spacing of $d = 39$ nm is found at $w_{pol} = 35$ wt. %, which increases smoothly with increasing polymer concentration. Interestingly, after preparation the microdomain structure appears to be highly oriented parallel to the electrodes. This can be seen from the two-dimensional SAXS pattern displayed in Fig. 1(b), which shows two distinct peaks around $\varphi = 0°$ and $\varphi = 180°$. This behavior is retained after heating the sample above the order-disorder temperature and subsequent cooling. We therefore anticipate that preferential attraction of the PS block to the gold surfaces is responsible for this alignment [18].

When an electric field is applied across the two electrodes, the scattering pattern changes significantly. As can be seen from the snapshots taken at different times, the anisotropic pattern first turns into an isotropic ring of weak intensity [Fig. 1(c), $t = 6$ s] before two distinct peaks are formed at about $\varphi = 90°$ and $\varphi = 270°$ at later times [Fig. 1(d), $t = 34$ s]. The complete set of data is displayed in Fig. 2(a), where the intensity of the (1 0 0) peak is plotted as a function of φ for increasing time t. Clearly, an almost complete destruction of the initial peaks is seen at early times followed by the buildup of new peaks at about $\varphi = 90°$ and $\varphi = 270°$.

Before we turn to a quantitative discussion of the kinetic data, we note that a qualitatively different reorientation behavior is observed when the polymer concentration is significantly increased. This is shown in Fig. 2(b) for a polymer solution with $w_{pol} = 50$ wt. %. In contrast to the situation described above, the initial scattering peaks are not destroyed as the electric field is applied; however, they merely rotate from their original positions at $\varphi = 0°$ and $\varphi = 180°$ towards their final positions at $\varphi = 90°$ and $\varphi = 270°$, respectively. The peak intensities decrease slightly during the rotation process and eventually increase again after the final orientation has been reached. For intermediate concentrations (not shown here), a superposition of both behaviors is observed. Interestingly, we can retain the original mechanism, if we increase the temperature. This can be seen in Figs. 2(c) and 2(d), where the reorientation behavior of a sample with $w_{pol} = 47.5$ wt. % is shown at two different temperatures. While a shift of the peaks dominates at lower temperatures [$T = 27$ °C, Fig. 2(c)], a destruction of the initial signals is followed by a buildup of two new peaks at well-defined positions at about $\varphi = 90°$ and $\varphi = 270°$ at higher temperatures [$T = 80$ °C, Fig. 2(d)]. Again, at intermediate temperatures both behaviors coexist.

These findings point to two different underlying mechanisms responsible for microdomain reorientation in the presence of the electric field. Close to the ODT, i.e., at low concentrations and high temperatures, microdomains aligned parallel to the electric field grow at the expense of those aligned parallel to the electrodes. Intermediate orientations, however, are not observed.

This behavior matches the notion of the migration of grain boundaries [Fig. 3(a)], which has previously been described for microdomain alignment under shear [16] and which was assumed to play a role in electric-field experiments as well [9,10,19]. As indicated in Fig. 3(a), one lamella grows at the expense of another with a significantly different orientation by motion of a tilt boundary (wall defect) between them, leading to a direct transfer of scattering intensity between widely separated azimuthal angles φ.

Further away from the ODT, i.e., for high concentrations and low temperatures, the scattering pattern seems to be preserved and merely shifts into the new orientation. This observation points to the rotation of entire grains as an alternative orientation process [Fig. 3(b)]. The grains exhibit a broad size distribution ranging between a few to some hundred microns as determined by polarization optical microscopy (not shown here). In contrast to the migration of grain boundaries, microdomain orientations intermediate between the initial and the final orientations are observed. At the same time, no increase in isotropic scattering is detected. Nevertheless, the peak intensity decreases temporarily and is recovered only after the final orientation is reached. This decrease indicates that the grains do not necessarily rotate around the x-ray beam direction, but rather in a way where they do not contribute to the scattering signal. This is in contrast to mechanical shear fields, which impose a preferential axis of domain rotation. The observation that all grains rotate in the same sense towards their final orientation is possibly induced by slight misorientations of the initial states due to misalignment of the sample. The fact that the final orientation parallel to the electric-field vector is not fully reached within the experimental time frame is in agreement with the notion that the driving force for grain alignment almost vanishes as the aligned state is approached [10].

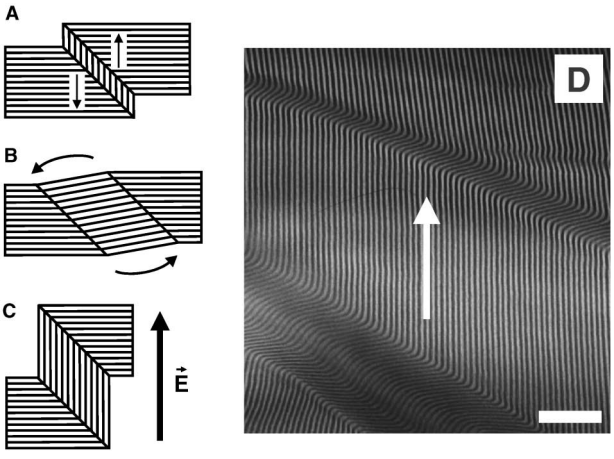

FIG. 3. Sketch of the two dominating microscopic mechanisms: (A) grain boundary migration and (B) grain rotation, eventually leading to an alignment parallel to the electric field (C). (D) TEM picture of a typical kink band defect observed after electric-field alignment. Scale bar = 400 nm.

We note that the observed behavior near ODT may also indicate what is typically referred to as the dissolution/reformation mechanism ("selective melting") [20,21]. This mechanism would involve partial dissolution of microdomains (at the size of several microns) which are perpendicular to the external field, followed by creation of domains parallel to the electric field. However, since we did not detect any shifts in the ODT induced by the electric field, we do not expect electric-field-induced mixing of PS and PI. In addition, no radial broadening (q dependence) of the scattering intensities is observed during the reorientation process. We therefore tend to exclude microdomain "melting" as a relevant mechanism in our experiments, whereas we anticipate that for migration of grain boundaries it may play a role on a molecular level, as in principle single chain motion is sufficient to stepwise change the orientation of large areas along a wall defect ("molecular scale reorientation"). Our mechanistic picture is further corroborated by typical kink band defects found in bulk samples prepared by solvent casting under an applied electric field [Fig. 3(d)].

We note that the integrated scattering intensity in Fig. 2 slightly drops during the initial stage of the reorientation process and is found to increase at later times (not shown here). The initial decrease may result from lamellae rotating out of the plane of observation. The eventual increase, on the other hand, indicates the overall growth of domains at later times.

The transition from grain rotation to migration of grain boundaries on approaching ODT can be explained by the fact that at high concentrations and low temperatures, i.e., in a strongly segregated system, grain boundaries are thermodynamically unfavorable. Therefore, larger grains are formed which exceed a certain critical size, so that they can be rotated effectively by the electric field. This has already been anticipated for diblock copolymer melt systems [19]. At low concentrations and high temperatures, i.e., in a weakly segregated system, the energetic penalty for the creation of boundary interfaces is much lower. Furthermore, close to ODT, we also expect a high defect density and mobility. The vast majority of grains formed are obviously not large enough to be rotated by the electric field. On the other hand, the mobility of defects such as grain boundaries (wall defects) is large, which allows the system to orient its domains parallel to the electric field by single chain based migration of grain boundaries.

A quantitative evaluation of the domain boundary migration process proves difficult due to the overall intensity variations mentioned above. The grain rotation process, however, is reflected in an intensity independent change of the scattering angle, which is unambiguously extracted from the data. For this end, we model the azimuthal scattering intensity at about $\varphi = 180°$ by two Gaussians, one fixed at the initial peak position and the other one being allowed to shift towards the final position as a function of time. We reveal the respective peak intensities

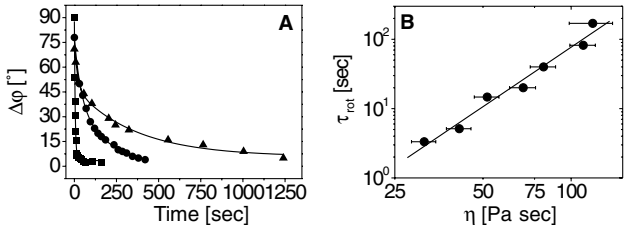

FIG. 4. (A) Angular shift of rotational component at different concentrations ($\square = 35$ wt. %, $\bigcirc = 47.5$ wt. %, $\triangle = 50$ wt. %) at field strength of $E = 1$ kV/mm at $T = 25\,^{\circ}$C. The solid lines represent least-squares fits to the data yielding the rotational time constant τ_{rot}; (B) bilogarithmic plot of τ_{rot} versus solution viscosity, η.

and the position of the maximum, $\Delta\varphi$, of the shifting peak from least-squares fits to the experimental data. Figure 4(a) shows the position of the shifting peak $\Delta\varphi$ versus time for different copolymer concentrations. The data in Fig. 4(a) can be fitted by a single exponential (solid lines) yielding an effective rotational time constant τ_{rot}. This time constant describes the average kinetics of the rotation of entire grains of different sizes. One may assume that this microscopic measure should somehow scale with the macroscopic viscosity, η, of the block copolymer solution. Therefore, we determined the solution viscosity η at 1 rad/s for different concentrations using a Rheometrics Stress Rheometer SR-5000 with a plate-plate geometry (diameter: 25 mm). Both frequency and time sweeps were performed and the final values are averages over at least three independent measurements. With these data, we can establish a relation between the (microscopic) rotational time constant τ_{rot} and the (macroscopic) viscosity η of our block copolymer solutions. A bilogarithmic plot of τ_{rot} versus η [Fig. 4(b)] yields a straight line with a slope of 2.85 ± 0.22 indicating a power law behavior $\tau_{rot} \propto \eta^{2.85\pm0.22}$.

We note that the dependence of τ_{rot} on polymer concentration will result from a subtle balance between the driving force of the electric field and some sort of viscous retardation. The former is expected to grow with increasing polymer concentration as both the dielectric contrast and the degree of incompatibility will increase. At the same time, the solution viscosity is growing with polymer concentration. The exact behavior is difficult to predict; however, the data shown in Fig. 4(b) indicate that in the particular system studied here the increase in viscosity dominates over the increase of the driving force.

In conclusion, we have shown that real-time synchrotron SAXS measurements provide insight into the microscopic processes relevant for microdomain alignment in concentrated block copolymer solutions. Close to the ODT, migration of grain boundaries seems to be the governing mechanism, while rotation of grains dominates further away from the ODT, i.e., under strongly segregating conditions. The rather fast reorientation kinetics could be nicely resolved and were quantified separately by extracting the time constant for the rotational component, τ_{rot}. Provided that a quantitative model for the dependence of τ_{rot} on the solution viscosity can be established, the determination of rotational time constants can provide microscopic insight into the local dynamics of block copolymer solutions.

The authors thank H. Krejtschi and his team for skillful assistance in building the capacitors, K. Matussek for the viscosity measurements, A. Göpfert for operating the TEM, and H. Schmalz for cooperation during the block copolymer synthesis. We are grateful for many helpful discussions with H. Brand. A. B. acknowledges the Verband der Chemischen Industrie (VCI) and the BMBF. We thank the ESRF for financial support and provision of synchrotron beam time. This work was carried out in the framework of the Sonderforschungsbereich 481 funded by the Deutsche Forschungsgemeinschaft (DFG).

*Electronic address: georg.krausch@uni-bayreuth.de

[1] F. S. Bates and G. H. Fredrickson, Annu. Rev. Phys. Chem. **41**, 525 (1990).
[2] F. S. Bates and G. H. Fredrickson, Phys. Today **52**, No. 2, 32 (1999).
[3] U. Wiesner, Macromol. Chem. Phys. **198**, 3319 (1997).
[4] Z.-R. Chen, J. A. Kornfield, S. D. Smith, J. T. Grothhaus, and M. M. Satkowski, Science **277**, 1248 (1997).
[5] A. Keller, E. Pedemonte, and F. M. Willmouth, Science **225**, 5232 (1970).
[6] R. J. Albalak and E. L. Thomas, J. Polym. Sci., Part B: Polym. Phys. **31**, 37 (1993).
[7] S. Stangler and V. Abetz, e-Polymers **018** (2002).
[8] T. Thurn-Albrecht, J. DeRouchey, T. P. Russell, and H. M. Jaeger, Macromolecules **33**, 3250 (2000).
[9] K. Amundson, E. Helfand, X. Quan, S. D. Hudson, and S. D. Smith, Macromolecules **27**, 6559 (1994).
[10] K. Amundson, E. Helfand, X. Quan, and S. D. Smith, Macromolecules **26**, 2698 (1993).
[11] T. L. Morkved, M. Lu, A. M. Urbas, E. E. Ehrichs, H. M. Jaeger, P. Mansky, and T. P. Russell, Science **273**, 931 (1996).
[12] J. Le Meur, J. Terrisse, C. Schwab, and Goldzene, J. Phys. (Paris), Colloq. **5**, 301 (1971).
[13] A. Böker, A. Knoll, H. Elbs, V. Abetz, A. H. E. Müller, and G. Krausch, Macromolecules **35**, 1319 (2002).
[14] N. P. Balsara and B. Hammouda, Phys. Rev. Lett. **72**, 360 (1994).
[15] K. I. Winey, S. S. Patel, R. G. Larson, and H. Watanabe, Macromolecules **26**, 4373 (1993).
[16] D. L. Polis, S. D. Smith, N. J. Terrill, A. J. Ryan, D. C. Morse, and K. I. Winey, Macromolecules **32**, 4668 (1999).
[17] Y. M. Zhang and U. Wiesner, J. Chem. Phys. **103**, 4784 (1995).
[18] S. H. Anastasiadis, T. P. Russell, S. K. Satija, and C. F. Majkrzak, Phys. Rev. Lett. **62**, 1852 (1989).
[19] K. Amundson, E. Helfand, D. D. Davis, X. Quan, S. S. Patel, and S. D. Smith, Macromolecules **24**, 6546 (1991).
[20] F. A. Morrison and H. H. Winter, Macromolecules **22**, 3533 (1989).
[21] D. B. Scott, A. J. Waddon, Y. G. Lin, F. E. Karasz, and H. H. Winter, Macromolecules **25**, 4175 (1992).